Kovove Mater. 52 2014 237–242
DOI: 10.4149/km_2014_4_237

Weldability of AA6063 alloys by using Keyhole Gas Tungsten Arc Welding technique

T. Teker[1], T. Kurşun[2]*

[1] *Department of Materials Engineering, University of Adıyaman, Adıyaman 02040, Turkey*
[2] *Department of Manufacturing Engineering, University of Cumhuriyet, Sivas 58140, Turkey*

Received 9 May 2012, received in revised form 24 June 2014, accepted 19 May 2014

Abstract

This study shows that Keyhole Gas Tungsten Arc Welding (KGTAW) process enabling a single pass of 10 mm thick AA6063 alloy can be used without expensive filler metal addition or joint preparation. KGTAW has significantly high productivity as well as simplicity of proven technology and low capital investment requirements. It can be successfully applied in the welding of AA6063, without sacrificing the metallurgical quality associated with the Gas Tungsten Arc Welding (GTAW) process. After KGTAW, to determine the microstructural changes and to observe phases and compounds generated on the interface, welded samples were examined by OM, SEM and XRD. In addition, microhardness, tensile and notch impact strength tests were applied to determine the mechanical properties of welded samples (S1, 550 A and S2, 600 A). The best result was obtained for the S2 sample in the KGTAW technique.

Key words: Keyhole Gas Tungsten Arc Welding (KGTAW), AA6063, mechanical properties

1. Introduction

Aluminum and its alloys have important advantages at aerospace, automotive industries and in many structural applications because of their higher specific mechanical strength, corrosion resistance, light weight. AA6063 alloy is among the most widely used aluminum alloys among 6000 series. In this alloy, all the elements and impurities increase the strength of aluminum in various degrees [1–5].

The alloys are sensitive to weld metal cracking, particularly when the weld metal is rich in parent metal such as in the root pass of the weld. Fortunately, the cracking can be readily prevented by the use of filler metals containing higher proportions of silicon such as 4043 or the higher magnesium alloys such as 5356. Welding without filler metal or with filler metal of parent metal composition is rarely practized because of the risk of weld metal hot cracking. A weld metal with a composition close to that of the parent metal may age-harden naturally or it may be artificially aged to achieve strength close to that of the aged parent metal. In the overheated zone in the Heat Affected Zone (HAZ) closest to the fusion line, partial melting of the grain boundaries takes place. Temperatures are high enough and cooling rates are sufficiently fast so that the solution treatment takes enabling some aging to occur after welding. In the partially solution-treated zone where some of the precipitates are taken into solution, post-weld hardening occurs, but the precipitates that do not dissolve coarsen. The zone where precipitate coarsening takes place overages and there is a large drop in strength [6–8]. Tungsten Inert Gas (TIG) process tends to be limited to the thinner gauges of aluminum, up to approximately 6 mm in thickness. It has a shallower penetration into the parent metal than Metal Inert Gas (MIG) process and difficulty is sometimes encountered penetrating into corners and into the root of fillet welds [6].

Conventionally, the high current GTAW process is operated in the melt-in mode. In this mode process performance is enhanced through displacement of the weld pool, and this allows the thermal energy to be delivered efficiently to the interior of the weldment. The pool displacement is a result of a quadratic depend-

*Corresponding author: tel.: +90 349 2191241; fax: +90 349 2191241; e-mail address: tkursun08@gmail.com

Table 1. Chemical composition of material used in experiments

Alloy	Alloy elements (wt.%)						
	Cu	Fe	Si	Zn	Mn	Mg	Al
AA6063	0.15	0.6	0.8	0.1	0.1	1.1	Bal.

ence of arc force on the welding current. However, at higher currents, these forces can destabilize the pool, thereby limiting the operating window for the application. One solution is to modify the process parameters for reducing the overall arc force and distributing it more evenly over the liquid metal. In effect, this can be equated to the reduction of the peak arc pressure [9].

A recently introduced alternative solution is to increase the peak arc pressure and adjust the process parameters in order to puncture a small opening through the root face of the plate [10–11]. Provided the opening is kept small, the resulting keyhole will close behind the arc and the weld will be completed. The successful generation of keyhole mode GTAW is dependent on a number of process variables including the physical properties and dimensions of the plate, tungsten electrode geometry, shielding gas composition, arc voltage, welding current and travel speed. Nevertheless, for a given material and well chosen electrode geometry, the operating windows are often very robust and variations to current and travel speed may be all that is required to adjust the process over a significant range of plate thickness. In practice, the welding speed is selected first and the current is then adjusted, often visually, to form a reliable keyhole.

In this paper, we have examined the applicability of the KGTAW process to AA6063 in an effort to minimize the number of weld passes required for joint completion. The emphasis was placed on the thorough evaluation of the microstructure and mechanical properties.

2. Material and method

Commercially available similar AA6063 plates were used in experiments. The results of chemical analyses of this material are listed in Table 1. The mechanical properties are also given in Table 2.

The test pieces were clamped to a purpose-built welding platform and the assembly was driven past the stationary GTAW torch by the action of a single-axis translation stage. A lanthanated tungsten electrode, 6.4 mm in diameter with a 60° tip, was used for the welding. The electrode-to-plate separation was manually set to 1 mm prior to commencing each weld. Current was supplied from a conventional GTAW power source (UMS AC-DC TIG 350). Current and voltage were measured at the power source. The optimum welding parameters were determined by performing a series of bead-on-plate trials and examining the bead profile. The optimized parameters are presented in Table 3.

Two plates, each $400 \times 200\,\mathrm{mm}^2$ in dimension, were used to prepare the butt weld test plate. The square edges were machined and thoroughly degreased using acetone. The edges were in contact with each other so that there was no joint gap. No filler wire was used. The test plates produced using two KGTAW processes were sectioned transverse to the weld direction for general microstructural characterization. For metallographic examination, the welded specimens were cut transversely through the bond using a low-speed saw. This involved grinding with various grades of silicon carbide papers followed by polishing using 15 mm diamond grit. A final polishing was carried out with colloidal silica containing 2 % hydrogen peroxide and 2 % ammonia. The samples were etched with both Kroll's reagent (5 % nitric acid and 1 % hydrofluoric acid in water).

Microstructural changes on welding interface were examined by optical microscopy (OM) and scanning electron microscopy (SEM: JEOL JSM 7001) device. Energy dispersive spectrometry (EDS) analysis was done by JEOL JSM 7001 SEM type device to pick up

Table 2. Mechanical properties of material used in experiments

Alloy	Tensile strength (MPa)	Yield strength (MPa)	Hardness HV	Impact strength (J)
AA6063	90	48	75	12

Table 3. Parameters used in KGTAW

Sample No.	Filler wire	Current (A)	Voltage (V)	Travel speed ($\mathrm{m\,min^{-1}}$)	Shielding gas ($\mathrm{l\,min^{-1}}$)	Process
S1	None	550	16	0.02	15	KGTAW
S2	None	600	16	0.02	15	KGTAW

the elementary contents of phases which were formed at the interface appearance of the welded samples. Microhardness measurements of samples were carried out at an interval of 0.5 mm on load of 5 g with HV hardness scale. Lecia MHT-10 testing machine was used for microhardness measurements. In order to determine the phases and compounds on samples, XRD analysis was carried out through SHIMADZU XRD-6000 equipped with a Cu Kα/tube, wave length λ of 1.54056 A, voltage of 40 kV and ampere of 40 mA. Impact test samples were prepared for the mechanical examination of the welds. ASTM E23-04 specifications were followed for preparing and testing the impact samples [12]. Then, the samples were tested using a Wolpert PW30 notch Charpy test device with a hammer of 300 J. Tensile test samples were processed in a milling machine according to the measures ASTM E8M-04 guidelines [13]. The tensile strength of samples was determined by a Hounsfield tensile test machine with a capacity of 50000 N and 1 N accuracy and speed of 2 mm min^{-1}.

3. Results and discussion

3.1. Microstructure evaluation

Figure 1 shows the width of welding surface realized by KGTAW process using one nozzle diameter. From the figure, the widths of welding surface (S1, S2) are seen as approximately 8 and 10 mm for the KGTAW, respectively. Figures 2a,b show the penetration depth of the samples S1, S2 (without material) which were joined by KGTAW process with different parameters. The penetration depths in the samples S1, S2 were obtained as 6 and 7 mm (Fig. 2). The results show that welding current is an important parameter in the KGTAW. For 600 A energy input is more intensive than 550 A, thus the welding penetration is higher. Figure 3 shows a low magnification light optical micrograph of the KGTAW weld for S2. The variation in microstructure as one moves from the weld metal, through the HAZ on to the fusion zone, along a line just below the weld top is observable. It is seen that the solidification begins from the grains of the basic metal and continues toward the center of the weld metal in the form of dendrites. The weld metal grains of the joints, in which the alternative current is used as a conventional method in aluminum and alloys, were formed as very large dendrites and alpha aluminum grains (white areas) became dominant in the structure.

In the literature [5, 6], it is stated that large grains like column occur in welding seams performed without using pulse current. This is because the heat input is high, the weld metal pool is large, and as a result, the solidification is slow. High magnification SEM was used to observe the effect of welding parameters on coarse precipitation in the matrix and at grain boundaries within the HAZ of welds (Fig. 4). Although the KGTAW weld was deposited with a higher heat input for the single pass than that used for each run in the

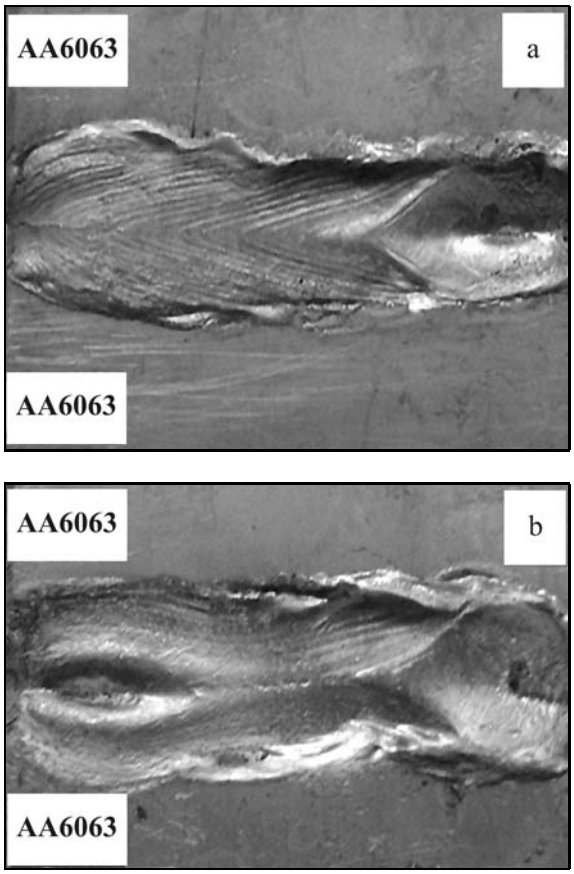

Fig. 1. The surface macro appearance of the S1 and S2 samples.

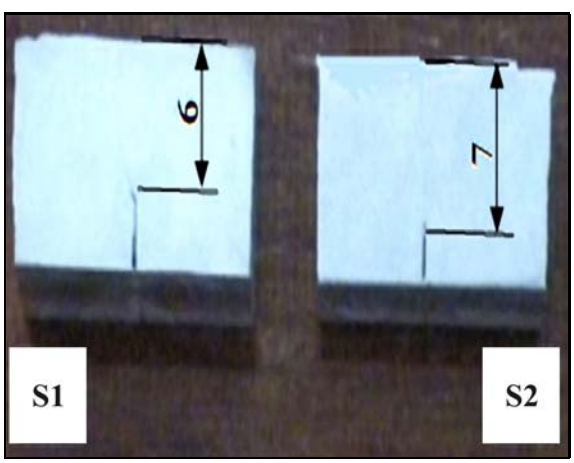

Fig. 2. The cross-sectional macro appearance of the samples S1 (a) and S2 (b).

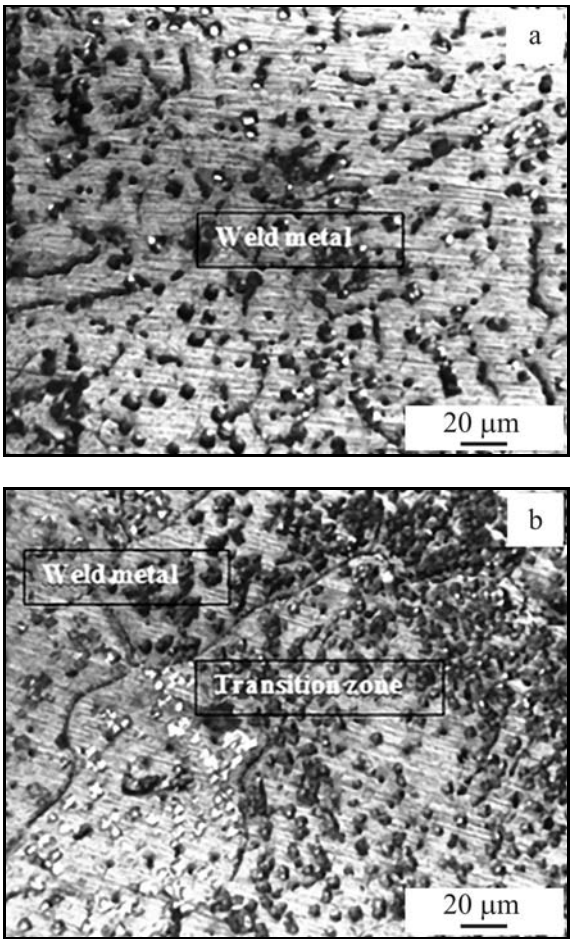

Fig. 3. Optical micrograph taken from the welding interface of S2 sample: weld metal (a) and side of AA6063 and transition zone (b).

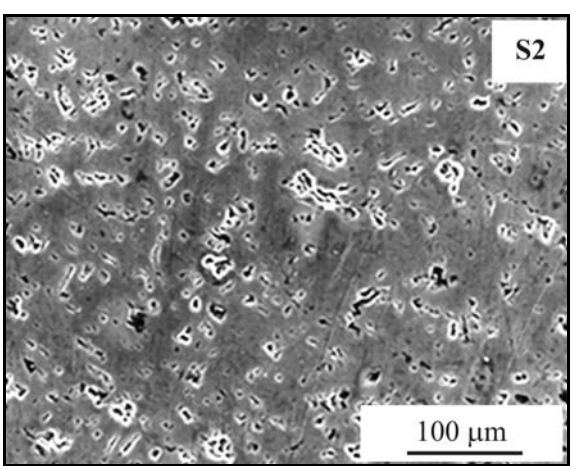

Fig. 4. Weld metal SEM photograph of the S2 sample.

conventional GTAW weld, it is seen that the columnar grains in the fusion zone of the two welds have similar coarse grain sizes. However, the HAZ of the KGTAW

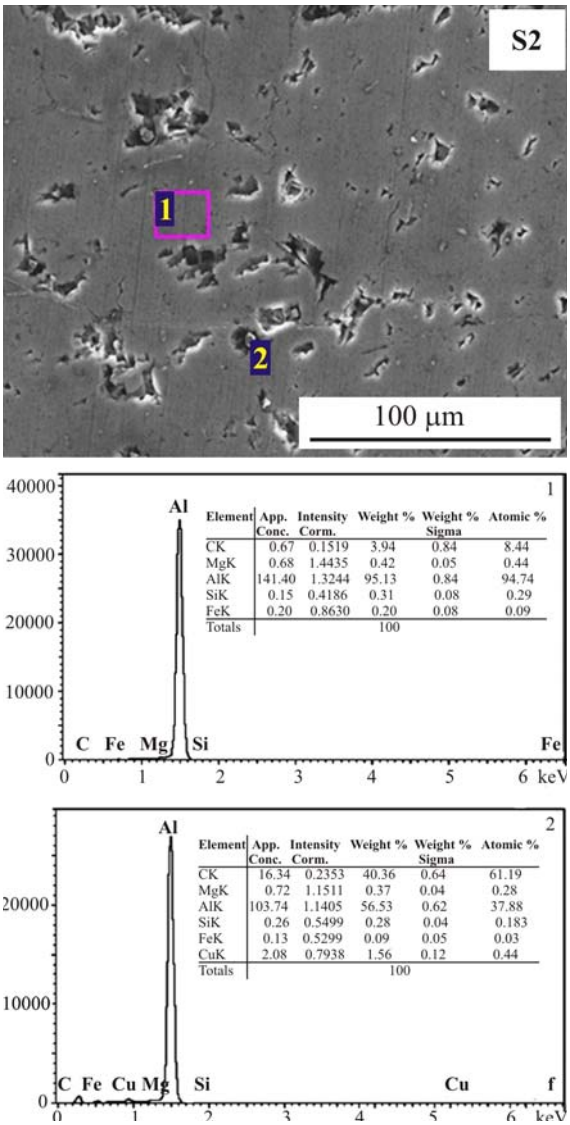

Fig. 5. EDS analysis of S2 sample.

weld is significantly wider. No pores, fissures and incomplete fusion of filler are observed in the central zone of weld, and the structure is dense and transits naturally nearby the weld junction, showing that the fluidity of molten pool is improved significantly by the AA6063 alloy. It is seen that significant grain coarsening has occurred in the HAZ immediately adjacent to the base material and the degree of grain coarsening increases as one moves.

Figure 5 shows the SEM micrograph and EDS results of S2. The point 1 on sample S2 consists of 95.13 % Al, 0.42 % Mg, 0.31 % Si. The point 2 consists of 56.83 % Al, 0.37 % Mg, 0.28 % Si. The result of EDS analyses of S2 sample in Fig. 4 reveals that Al and Mg element diffusions were originated from AA6063 through weld metal. This composition was detected as Al-Si eutectic from the Al-Mg-Si ternary phase dia-

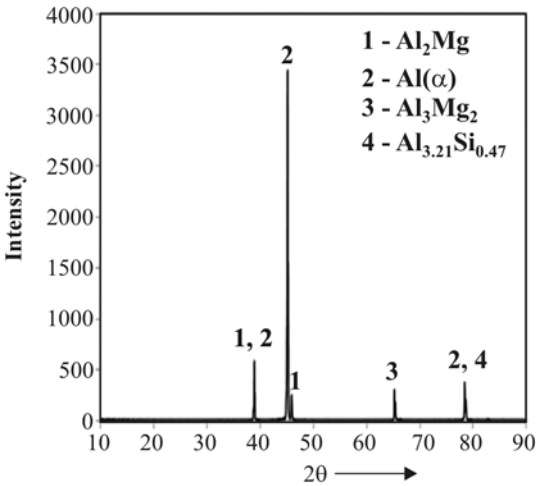

Fig. 6. XRD analysis of S2 sample.

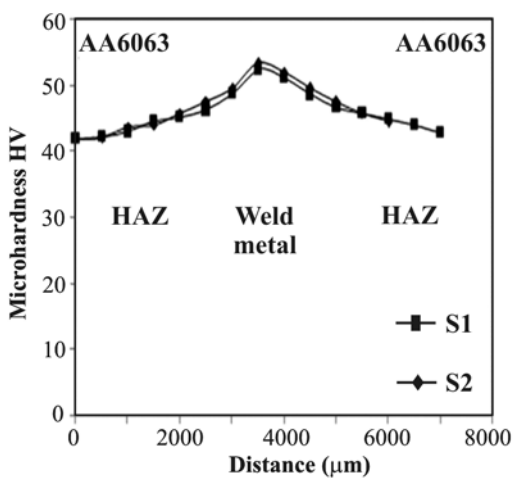

Fig. 7. Microhardness distribution across the welding interface of KGTAW welded samples.

gram. Also, from the microstructure in Fig. 5, Al-Si ötectic and Al(α) are seen in the matrix. Finally, the results of EDX analysis performed across the welds confirmed the information given by the correlation analysis of the spectra. We observed that the magnesium lost along the weld axis was not uniform in the keyhole mode welding.

The phases and compounds occurred in samples were determined by X-ray analyses. Figure 6 shows the X-ray diffraction analyses of S2 sample. The XRD results of S2 sample indicated the presence of Al(α), Al_2Mg, Al_3Mg_2, $Al_{3.21}Si_{0.47}$.

3.2. Hardness tests

The microhardness analyses of welded joints on S1 and S2 are given in Fig. 7. The hardness values of S1 and S2 at welding center are 53.1 HV and 51.2 HV, respectively.

The 75 HV hardness value of the main material was used in the experimental study. The alpha aluminum occuring in the weld metal of S1 and S2 samples, which are obtained using alternative current, formed large dendrites and decreased the hardness value due to the intensity (increase) of heat input and the length of the solidification period. According to EDS (Fig. 5) and XRD (Fig. 6) results, the causes of high microhardness value at weld seam were Al(α), Al_2Mg, Al_3Mg_2, $Al_{3.21}Si_{0.47}$ phases and compound emerging due to instantaneous cooling.

3.3. Mechanical properties

According to the results of the tensile test, the tensile stress values of S1 and S2 were 69.5 and 117.9 N mm^{-2}, respectively. The values of elongation were 4.5 and 6.7 % for S1 and S2 samples, respectively. It is seen that the tensile strength of the main material used in the experimental study was 90 MPa, the strength of the material combined using pulse current was 5 MPa, and the tensile strength for S2 using KGTAW method was 117.9 MPa.

During the tensile test, materials were broken on weld metal side without elongation and being wasted. The previous investigations show that the maximum tensile strength of welded joint by a single pass AC-TIG weld in a 6061 series alloy made with a 4043 filler metal was approximately 300 N mm^{-2} in the post-weld aged condition and the maximum tensile strength of multi-pass MIG weld made with a 4043 filler was approximately 230 N mm^{-2} [14]. Remarkably, high-quality weld in favor of improving the mechanical properties of welded joint was produced by KGTAW of AA6063 alloys in the post-weld aged conditions.

In order to assess the toughness of the welded joints, notch Charpy 'v' tests were performed. The notch Charpy test results of S1 and S2 samples at room temperature indicated that the highest Charpy toughness was developed on S2 sample with a value of 15 J, while the lowest value, 9 J, was developed on S1 sample. When the results were examined, it was seen that the impact strength of the main material used in the experimental study was 13 J, and the weld metal strength of the material combined using KGTAW method compared with the main material, the weld metal strength of the materials combined using KGTAW method enhanced about 15 % value.

Normally, due to the welding heat, AA6063 exhibited overaging of the precipitates or coarsened grain structure at the weldment, which could be the reason for a reduction in toughness of the joints. Toughness can be regained only by refining the grain size through cold working and annealing. Concurrently, depending on increasing current intensity, an increase is noticed

in the notch impact values of the welded joints. This may be attributed to the fact that the penetration depth goes up due to higher temperatures and energy density resulted from increasing current intensity and a rise in heat.

On the other hand, lower heat inputs are preferable for precipitation hardened aluminum alloys in developing good mechanical properties. At the same time the heat input should be sufficient enough to produce defect free process zones along with a recrystallized and refined microstructure. The analysis of the process parameters reveals that a decrease in the penetration deep results in a drop in the notch impact toughness values. This may be correlated with the presence of cavities and unwelded zones developed across the welded joints which led to stress concentration and reduced the toughness of the material by creating a notch effect due to declining penetration depth depending on gradually increasing welding current.

4. Conclusions

In this paper, we have shown that:

1. 10 mm thick, AA 6063, could be successfully welded in a single run using the KGTAW process, without special edge preparation or the addition of filler immediately evident. The evaluation of the microstructure-mechanical property relationships of the welded joints prepared by the keyhole processes then enabled a comparison of their metallurgical quality.

2. The higher heat input of the single pass of the KGTAW process and the associated weld thermal cycle with slower heating and cooling rates resulted in a wider HAZ. In both cases, a microstructure consisting of large dendrites and alpha aluminum grains was observed in both the weld metal and HAZ.

3. The tensile and impact strength of the welded samples without filler wire by KGTAW process were obviously increased with penetration depth.

4. While the penetration depths of the samples were increased in consequence of the increase in the current intensity, the alpha aluminum occurring in the weld metal of S1 and S2 samples formed large dendrites due to the intensity of the heat input and the length of the solidification period. In return, this reduced the hardness value of the samples considering the hardness value of the basic material and hot cracks occurred.

References

[1] Arik, H., Aydin, M., Kurt, A., Turker, M.: Mat. & Des., *26*, 2005, p. 555. doi:10.1016/j.matdes.2004.07.017

[2] Lean, P. P., Gil, L., Urena, A.: J. of Mat. Proc. Tec., *143–144*, 2003, p. 846. doi:10.1016/S0924-0136(03)00331-5

[3] Praveen, P., Yarlagadd, P. K. D. V.: J. of Mat. Proc. Tec., *164–165*, 2005, p. 1106. doi:10.1016/j.jmatprotec.2005.02.224

[4] Panigrahi, S. K., Jayaganthan, R.: Mat. Sci. and Eng. A, *528*, 2011, p. 3147.

[5] Richard, W. D., John, S. V., Mark, T. S., Stan, G. P.: J. of Mat. Proc. Tec., *128*, 2002, p. 38. doi:10.1016/S0924-0136(02)00162-0

[6] Mathers, G.: The Welding of Aluminium and Its Alloys. Cambridge, Woodhead Publishing Limited 2002.

[7] Praveen, P., Yarlagadd, P. K. D. V., Kang, M. J.: J. of Mat. Proc. Tec., *164–165*, 2005, p. 1113. doi:10.1016/j.jmatprotec.2005.02.100

[8] Zhang, S., Jiang, F., Ding, W.: Mater. Sci. Eng. A, *490*, 2008, p. 208. doi:10.1016/j.msea.2008.01.033

[9] Creedy, F., Lerch, R. O., Seal, P. W., Sordon, E. P.: Trans. Am. Inst. Elect. Eng., *51*, 1932, p. 556. doi:10.1109/T-AIEE.1932.5056119

[10] Jarvis, B. L., Ahmed, N. U.: Sci. Technol. Weld. Join., *5*, 2000, p. 1.

[11] Jarvis, B. L., Barton, K. J., Ahmed, N. U.: Process for Keyhole Welding. WO9921677A1. Geneva, World Intellectual Property Organisation Publication of International Application 1999.

[12] ASTM International Standard E23-06. Standard Test Methods for Notched Bar Impact Testing of Metallic Materials. West Conshohocken, PA, ASTM International 2006.

[13] ASTM International Standard E8M-04. Standard Test Methods for Tension Testing of Metallic Materials. West Conshohocken, ASTM International 2004.

[14] Lei, Y., Yuan, W., Chen, X., Zhu, F., Cheng, X.: Trans. Nonferrous Met., *17*, 2007, p. 313. doi:10.1016/S1003-6326(07)60091-0